scientific reports

Check for updates

OPEN

TLR2 promotes the progression of diabetes mellitus with atherosclerosis via activating NLRP3 inflammasome and MyD88/NF-κB signaling pathway

Sisi Chen[1], Min Xie[1] & Yong Liu[2]✉

Atherosclerosis, a critical vascular complication frequently associated with diabetes mellitus, develops due to the synergistic effects of multiple pathological mechanisms. Toll-like receptor-2 (TLR2) has been identified as a key contributor to the progression of a wide range of disorders. The primary goal of this research was to investigate the functional role of TLR2 in the context of diabetes mellitus-associated atherosclerosis (DMA) and to delineate the molecular pathways underlying its effects. The study enrolled 30 DMA patients and 30 healthy individuals. An *in vitro* model of DMA was developed to mimic the disease state. TLR2 expression levels were measured using RT-qPCR, while pyroptosis rates were assessed via flow cytometry. Western blot analysis was utilized to determine protein expression levels. Co-immunoprecipitation was performed to assess the interactions between TLR2 and myeloid differentiation primary response 88 (MyD88). A DMA mouse model was established. Oil red O staining were used to assess the effect of TLR2 on lipid deposition. Elevated levels of TLR2 were observed in both clinical samples from DMA patients and the experimental DMA cell model. The DMA model exhibited reduced cell viability, increased pyroptosis rates, elevated levels of pyroptosis-related proteins, and higher concentrations of interleukin (IL)-1β and IL-18. These effects were reversed upon TLR2 inhibition. Furthermore, inhibition of TLR2 expression effectively blocked the activation of the MyD88/NF-κB signaling pathway. Conversely, TLR2 overexpression reduced cell viability, enhanced pyroptosis, and activated the MyD88/NF-κB pathway, effects that were counteracted by NF-κB inhibition. In in vivo study, silencing of TLR2 improved inflammation and atherosclerosis in diabetic mice. The results demonstrated that TLR2 drives the progression of DMA through the activation of the NLRP3 inflammasome and the MyD88/NF-κB signaling cascade. These findings suggested that TLR2 could be a promising target for therapeutic interventions aimed at treating DMA.

Keywords TLR2, Diabetes mellitus with atherosclerosis, NLRP3, MyD88/NF-κB

Diabetes is a metabolic disorder where the body either cannot produce enough insulin or cannot effectively use the insulin it produces, leading to elevated blood glucose levels and potential complications affecting various organs over time. Globally, DM is among the most prevalent and rapidly increasing diseases, with projections estimating that it will affect approximately 693 million adults by 2045[1]. A significant challenge in managing DM is the absence of early diagnostic methods, which often results in delayed treatment and an increased risk of severe complications[2]. Diabetes mellitus is associated with numerous complications, predominantly resulting from chronic hyperglycemia-induced vascular damage affecting both macrovasculature and microvasculature, which ultimately leads to multi-system dysfunction[3]. One such complication is atherosclerosis, a chronic inflammatory condition characterized by arterial wall thickening and lipid accumulation[4]. The development of atherosclerosis is influenced by multiple factors, with inflammation playing a central role[5]. Research has revealed a significant interaction between oxidative stress and inflammatory mechanisms in the pathogenesis and advancement of atherosclerosis associated with diabetes mellitus (DMA)[6]. Current treatments for DMA, including hypoglycemic

[1]Department of Endocrinology, Renmin Hospital, Hubei University of Medicine, Shiyan City 442000, Hubei Province, China. [2]Department of Gastroenterology, Renmin Hospital, Hubei University of Medicine, 39 Chaoyang Middle Road, Shiyan City 442000, Hubei Province, China. ✉email: liuqwest2024@163.com

agents, antithrombotic therapy, and weight management, have limited efficacy. Therefore, identifying novel therapeutic targets for DMA is crucial.

Toll-like receptors (TLRs) are a class of proteins that play a key role in the innate immune system by recognizing pathogen-associated molecular patterns (PAMPs) from microbes[7]. Upon activation, TLRs initiate signaling cascades that lead to the production of cytokines and other immune responses essential for host defense against infections[8]. Specifically, TLR4 has been shown to amplify inflammatory reactions in cardiomyocytes, whereas TLR2 and TLR4 collectively contribute to the development of atherosclerosis associated with infections[9]. TLR2, a cell surface receptor found in various immune and epithelial cells, is particularly significant in the pathogenesis of diabetic microvascular complications[10]. Recent studies have reported elevated TLR2 expression in monocytes and neutrophils of patients with bronchial asthma and type 2 DM[11]. The activation of TLR2 depends on its association with the adaptor protein myeloid differentiation factor 88 (MyD88)[12], which subsequently initiates the NF-κB signaling pathway. NF-κB, a family of transcription factors, plays a critical role in regulating a wide range of physiological functions and pathological processes[13]. The MyD88/NF-κB pathway has been extensively studied in diseases such as cancer, but its role in DMA remains poorly understood, warranting further investigation.

The main goal of this research was to examine the expression and functional role of TLR2 in DMA and to elucidate the molecular mechanisms involving the MyD88/NF-κB pathway. These findings may provide a foundation for developing innovative therapeutic strategies aimed at treating DMA.

Methods and materials

Bioinformatics analysis

The STRING database (version 11.5; https://cn.string-db.org/) was used to identify proteins that interact with TLR2 and construct a protein-protein interaction network.

Clinical sample collection

Ethical approval for this study was granted by the Institutional Review Board of Renmin Hospital, Hubei University of Medicine. The study included 30 DMA patients and 30 healthy controls, with DMA patients meeting the diagnostic criteria outlined in prior research[14]. All participants provided written informed consent before enrollment. After an overnight fast, approximately 10 mL of blood was collected from each participant via standard venipuncture into sterile plain tubes without anticoagulants. The blood samples were left undisturbed at room temperature for 60 min to allow clotting. Subsequently, the blood samples were centrifuged at 3500 rpm for 15 min. The clear supernatant, which is the serum, was carefully transferred into new sterile tubes for further analysis. Demographic and clinical information of the participants was summarized in S1[15].

Cell culture and treatments

The human cardiac microvascular endothelial cell line (HCMECs) was procured from Thermo Fisher (USA). The cells were cultured in DMEM (Procell) enriched with 10% heat-inactivated FBS (BasalMedia), 0.05 mM β-mercaptoethanol (Yuanye Biotechnology Co., Ltd., Shanghai, China), and 1% penicillin/streptomycin (BasalMedia). The cultures were maintained at 37 °C in a humidified environment with 5% CO_2. To create an *in vitro*model of DMA, HCMECs were treated with 50 mmol/L glucose and 50 μg/mL human oxidized low-density lipoprotein (oxLDL, Yeason Biotechnology Co., Ltd., Shanghai, China) for 48 h. To inhibit NF-κB, the cells were exposed to 10 μM BAY 11–7082(BAY, Yeason), a specific NF-κB inhibitor, for 48 h[16]. In addition, the cells were treated with MG132 (10 μM), a proteasome inhibitor, for 4 h.

Cell transfection

The short hairpin RNA targeting TLR2 (sh-TLR2), a non-targeting shRNA control (sh-NC), the pcDNA3.1-TLR2 overexpression construct, and the empty pcDNA3.1 vector were all obtained from Genecreate Biological Engineering Co., Ltd. (Wuhan, China). In transfection experiments, HCMECs were seeded in six-well plates at 1 × 10^5 cells/well and cultured to ~80% confluence. Transfection was conducted using Lipofectamine 3000 (Yeason), followed by a 48-hour incubation for gene expression modulation.

Flow cytometry

The evaluation of pyroptosis in HCMECs was conducted by measuring caspase-1 activity through flow cytometry, based on established methodologies[17]. In brief, a FAM-fluorochrome-labeled caspase inhibitor (FLICA) from a commercially available *in vitro* Caspase Detection Kit (ImmunoChemistry, USA) was used. Cells were co-stained with FLICA and propidium iodide (PI) and incubated at 37 °C for 1 h in the absence of light. Following two washes with a designated wash buffer, the samples were subjected to analysis using a flow cytometer (BD Biosciences, USA).

Isolation and quantification of RNAs

Total RNA was extracted from serum and cell samples with TRIzol reagent (Yeason) and then reverse-transcribed into cDNA using a commercial kit (Toyobo Biotechnology Co., Ltd., Shanghai, China). Subsequently, quantitative PCR (qPCR) was carried out using another Toyobo kit, following the manufacturer's protocol. Gene expression levels were analyzed and normalized using the $2^{-\Delta\Delta CT}$ method, with primers designed and synthesized by Ribo Biotechnology Co., Ltd. (Guangzhou, China).

Western blot

PProtein was extracted using lysis buffer (Yeason), and its concentration was measured by the Coomassie Brilliant Blue assay (Vazyme Biotechnology Co., Ltd., Nanjing, China). Samples containing 50 μg of protein were resolved

on a 10% SDS-polyacrylamide gel and transferred to a PVDF membrane. The membrane was blocked with 2% BSA for 1 h at room temperature, followed by overnight incubation with primary antibodies at 4 °C. After three TBST (Vazyme) washes, the membrane was treated with a secondary antibody for 1 h at room temperature. Protein bands were detected using an ECL solution (Yeason). The used antibodies included TLR2 (ab213676; 1:1000; Abcam, Cambridge, MA, USA), GAPDH (ab9485; 1:2500; Abcam), ASC (ab283684; 1:1000; Abcam), NLRP3 (ab263899; 1:1000; Abcam), GSDMD-N (ab215203; 1:1000; Abcam), MyD88 (ab133739; 1:5000; Abcam), NF-κB (ab32536; 1:5000; Abcam), phospho (p)-NF-κB (ab76302; 1:1000; Abcam), IκBα (ab32518; 1:5000; Abcam), ubiquitination (PTM-1107; 1:1000; PTM Biotechnology Co., Ltd., Hangzhou, China), rabbit anti-mouse IgG (ab6728; 1:10,000; Abcam), and goat anti-rabbit (ab6721; 1:10,000; Abcam).

Cell counting kit-8 (CCK-8) assay

Cell viability was assessed using the CCK-8 kit (Solarbio, Beijing, China). Cells were plated in 96-well plates at 1× 10^3 cells/well (triplicates per condition), incubated for 24 h, and treated with 10 μL CCK-8 for 2 h. Absorbance at 450 nm was measured with a microplate reader to evaluate viability.

Immunofluorescence (IF)

Cells were seeded on glass coverslips, fixed with 4% paraformaldehyde (Solarbio) for 15 min, and permeabilized with 0.1% Triton X-100 (Solarbio) for 10 min. After being blocked with 5% bovine serum albumin (Abcam) for 1 h at room temperature, the cells were incubated overnight at 4 °C with the primary anti-MyD88 antibody (ab133739; 1:500; Abcam). Following phosphate buffer solution (PBS) washes, cells were stained with Alexa Fluor 488-conjugated secondary antibody (ab150081; 1:1000; Abcam) for 1 h at room temperature in the dark. Nuclei were counterstained with 4',6-Diamidino-2-Phenylindole (DAPI; 5 μg/mL; Abcam) for 5 min. Coverslips were mounted with antifade medium and visualized using a confocal microscope (Leica, Wetzlar, Germany).

Co-Immunoprecipitation (Co-IP)

Cells were lysed in RIPA buffer supplemented with protease/phosphatase inhibitors (Yeason). After centrifugation (12,000 × *g*, 15 min, 4 °C), supernatants were pre-cleared with protein A/G beads (Abcam). For each reaction, 500 μg lysate was incubated with 2 μg anti-TLR2 (MA5-49111; 1:50; Thermo Fisher) or anti-MyD88 (MYD88-101 AP; 1:100; Thermo Fisher) antibody overnight at 4 °C, followed by 2 h incubation with protein A/G beads. Beads were washed four times with lysis buffer, and bound proteins were eluted in 2 × SDS loading buffer (Beyotime Biotechnology Co., Ltd., Shanghai, China). Samples were analyzed by Western blot using anti-MyD88or anti-TLR2antibodies.

IP

To analyze MyD88 ubiquitination, cells were lysed and centrifugated. Then, 1 mg lysate was immunoprecipitated overnight with 2 μg anti-MyD88 antibody at 4 °C, followed by protein A/G bead incubation for 2 h. Beads were washed 4 × with lysis buffer, and ubiquitinated proteins were eluted in 2 × SDS buffer. Samples were resolved by SDS-PAGE and immunoblotted with anti-ubiquitin antibody.

Animal study

Male C57BL/6 mice (8 weeks old; 20–25 g) were housed under specific pathogen-free conditions with controlled temperature (22 ± 2 °C), humidity (50 ± 10%), and 12-hour light/dark cycles, with *ad libitum*access to food and water. After one week of acclimatization, mice were divided into two groups: (1) control group fed standard chow diet; (2) model group receiving high-fat diet (HFD, 45% kcal fat, 1.25% cholesterol) for 12 weeks combined with intraperitoneal streptozotocin (STZ, 50 mg/kg/day for 5 consecutive days) to induce diabetes. Fasting blood glucose levels were measured on the 3rd, 6th and 10 th days. Fasting blood glucose > 11.1 mmol/L was considered to indicate diabetes[18]. Afterwards, diabetic mice were randomly divided into three groups: (1) model group (HFD/STZ); (2) model + Adeno-Associated virus (AAV)-shNC group receiving HFD/STZ treatment plus intravenous injection of AAV–scramble shRNA (1×10^{11} vg/mouse) at week 4; and (3) model + AAV-shTLR2 group receiving HFD/STZ treatment plus intravenous injection of AAV-shTLR2 (1×10^{11} vg/mouse) at week 4. At week 12, mice were fasted overnight and euthanized by CO_2. Then, serum was collected via cardiac puncture. Besides, aortic tissues were also collected for subsequent Oil Red O staining analysis. All procedures were approved by the Institutional Animal Care and Use Committee and conducted in accordance with NIH guidelines.

Enzyme-linked Immuno sorbent assay (ELISA)

The concentrations of TLR2, interleukin (IL)−18, and IL-1β were quantified using commercially available ELISA kits (Abcam) in accordance with the manufacturer's instructions.

Oil red O staining

Aortic tissues were fixed in 4% paraformaldehyde for 24 h at 4 °C, rinsed with PBS, and embedded in Optimal Cutting Temperature compound (Beyotime). Frozen Sect. (8 μm) were cut using a cryostat, mounted on slides, and air-dried for 30 min. Sections were then rinsed with 60% isopropanol for 5 min and stained with filtered Oil Red O working solution (0.5% in 60% isopropanol; Solarbio) for 15 min at room temperature. After differentiation in 60% isopropanol (30 s) and a distilled water wash, nuclei were counterstained with Mayer's hematoxylin (Solarbio) for 1 min. Slides were rinsed, mounted with aqueous medium, and imaged under a bright-field microscope.

Statistical analysis

Data analysis was conducted using SPSS 21.0 software (IBM Corp., Armonk, NY, USA). Results are presented as mean ± standard deviation. Comparisons between two groups were performed using Student's t-test. The diagnostic potential of TLR2 in DMA was evaluated through receiver operating characteristic (ROC) curve analysis. All statistical analyses, including ROC curve generation, were carried out using GraphPad Prism 9.0 (GraphPad Software Inc., San Diego, CA, USA; https://www.graphpad.com/). A p-value of less than 0.05 was considered statistically significant.

Results

Clinical characteristics of the study population

As presented in S1, the study included 30 healthy volunteers (age < 55: 14; age ≥ 55: 16; male: 11; female: 19) and 30 patients with DMA (age < 55: 18; age ≥ 55: 12; male: 21; female: 9). No significant differences were observed between the two groups in terms of age, gender, education level, smoking status, or alcohol consumption ($P > 0.05$).

TLR2 was increased in DMA patients

To investigate the role of TLR2 in DMA, we compared TLR2 expression levels between DMA patients and healthy controls. The results revealed a significant upregulation of TLR2 in DMA patients relative to the healthy group (Fig. 1A). Moreover, the ROC curve analysis indicated an AUC of 0.7789 for TLR2 (Fig. 1B), suggesting a potential association between TLR2 and DMA. ELISA results showed that compared with the healthy group, DMA patients showed increased serum TLR2 level (Fig. 1C).

TLR2 activated NLRP3 inflammasome in HCMECs

To explore the functional role of TLR2 in (DMA, an *in vitro* DMA model was developed. Results revealed a marked upregulation of TLR2 at both the mRNA and protein levels in the model group compared to controls (Fig. 2A and B). Besides, in comparison to the control group, model group mice showed increased serum TLR2 concentration (Fig. 2C). In addition, the model group also displayed decreased cell viability and an increased rate of pyroptosis compared to the control group (Fig. 2D and E). Moreover, elevated levels of pyroptosis-related proteins, including ASC, NLRP3, and GSDMD-N, as well as higher concentrations of IL-1β and IL-18, were observed in the model group relative to controls (Fig. 2F-H).

Association of TLR2 expression with clinicopathological characteristics in DMA

According to TLR2 mRNA expression, we divided 30 DMA patients into Low (N= 15) and High (N= 15) expression groups (S2)[15]. Results showed that compared with the Low group, High group patients showed higher systolic blood pressure (SBP) and diastolic blood pressure (DBP) as well as increased hemoglobin A1c (HbA1c), triglycerides (TG), total cholesterol (TC), low-density lipoprotein cholesterol (LDL-c), and uric acid (UA) concentrations. Besides, the high-density lipoprotein cholesterol (HDL-c) content was decreased in High group relative to the Low group. Moreover, the creatinine and alanine aminotransferase (ALT) contents between two groups showed no significant differences ($P > 0.05$).

Silencing of TLR2 reversed the results in model group

To further examine the influence of TLR2 on NLRP3 inflammasome activity and pyroptosis, TLR2 expression was silenced in the *in vitro* DMA model. RT-qPCR analysis confirmed a significant reduction in TLR2 mRNA levels following TLR2 knockdown (Fig. 3A). Notably, TLR2 inhibition restored cell viability, which was previously suppressed in the model group (Fig. 3B). Additionally, the elevated protein levels of ASC, NLRP3,

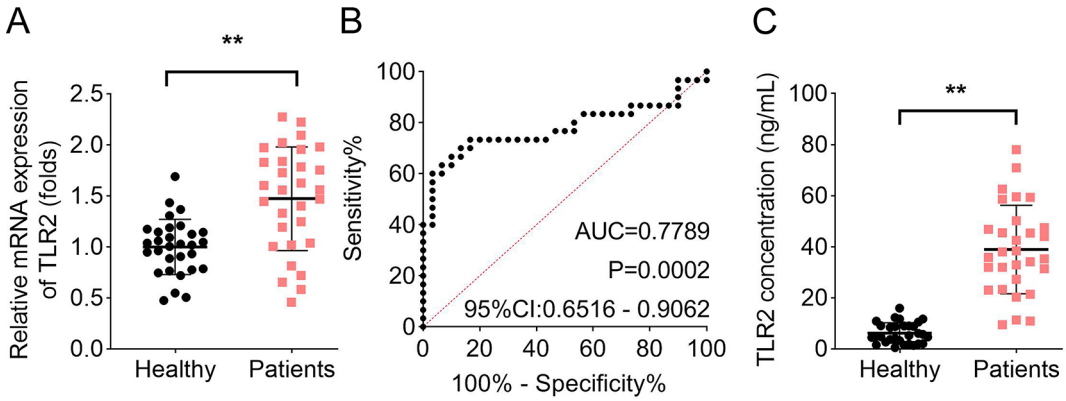

Fig. 1. TLR2 was increased in DMA patients. **A**, The expression of TLR2 in DMA patients and healthy volunteers was analyzed using reverse transcription-polymerase chain reaction assay; **B**, ROC curves of TLR2 in DMA; **C**, ELISA was performed to assess the serum TLR2 content in DMA patients and healthy volunteers. (**$p < 0.01$). TLR2, toll-like receptor 2; ROC, receiver operating characteristic; DMA, diabetes mellitus with atherosclerosis; ELISA, enzyme-linked immunosorbent assay..

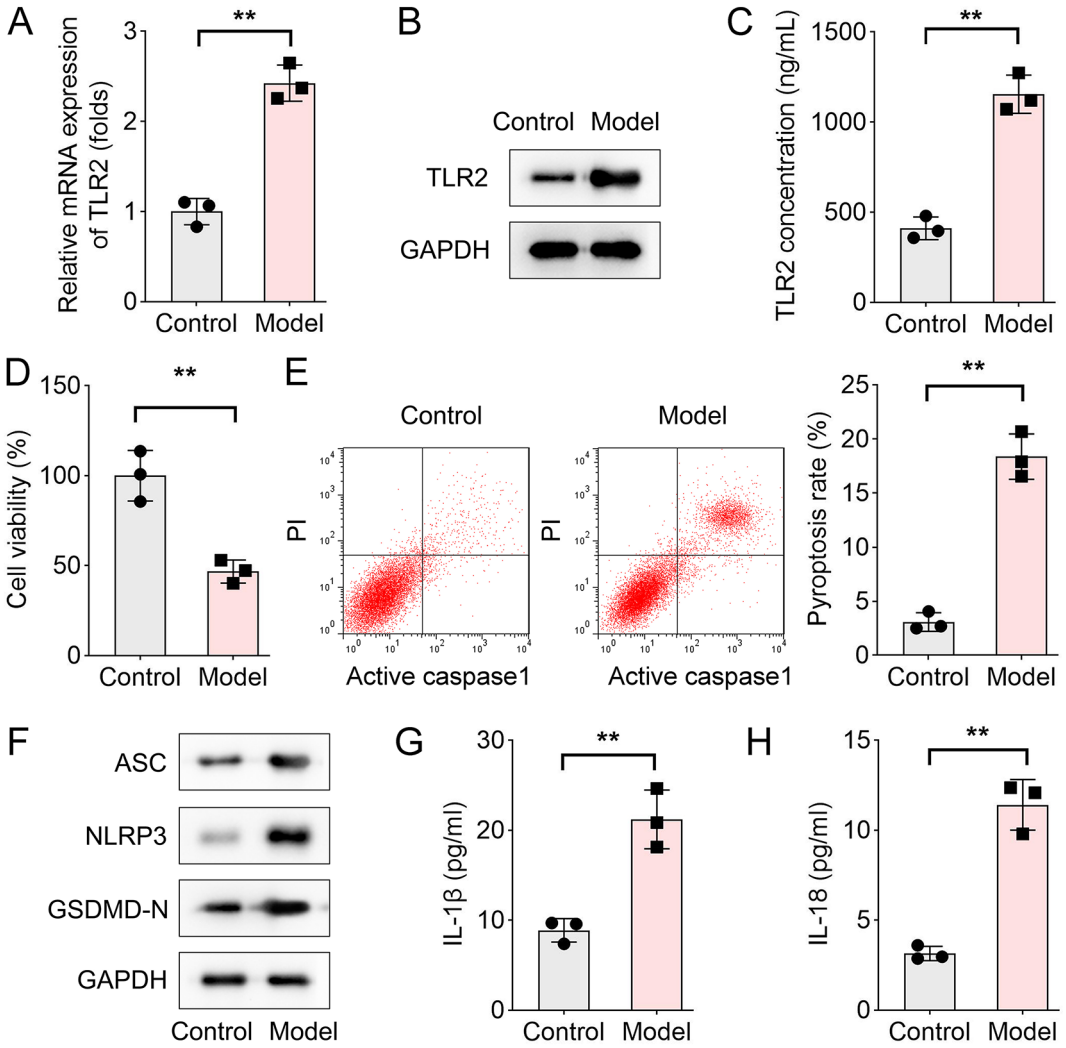

Fig. 2. TLR2 activated NLRP3 inflammasome in HCMECs. **A**, Reverse transcription-polymerase chain reaction was used to test the mRNA level of TLR2; **B**, The protein level of TLR2 was detected by Western blot; **C**, ELISA was performed to assess the serum TLR2 content in the control and model group mice; **D**, CCK-8 assay was used to detect the cell viability; **E**, Flow cytometry was conducted to assess the pyroptosis rate in control and model groups; **F**, Western blot was performed to analyze the protein levels of ASC, NLRP3, and GSDMD-N in control and model groups; ELISA was used to evaluate the concentrations of **G**, IL-1β and **H**, IL-18 in control and model groups. (**$p < 0.01$). TLR2, toll-like receptor 2; HCMECs, human cardiac microvascular endothelial cell line; ELISA, enzyme-linked immunosorbent assay; CCK-8, cell counting kit-8; ASC, apoptosis-associated speck-like protein containing a caspase recruitment domain; NLRP3, NOD-like receptor family pyrin domain containing 3; GSDMD, gasdermin D; ELISA, enzyme-linked immunosorbent assay; IL, interleukin.

and GSDMD-N observed in the model group were reversed upon TLR2 silencing (Figs. 3C-D). Furthermore, TLR2 knockdown led to a marked decrease in the pyroptosis rate and reduced concentrations of IL-1β and IL-18 compared to the model group (Figs. 3E-G).

Silencing of TLR2 inhibited MyD88/NF-κB signaling pathway activation in HCMECs

The STRING database was employed to map protein interactions involving TLR2, as depicted in Fig. 4A. Western blot results indicated higher levels of MyD88 and phosphorylated NF-κB (p-NF-κB) in the model group compared to controls, with these elevations being reversed upon TLR2 inhibition. In contrast, the expression of inhibitor kappa B alpha (IκBα) was lower in the model group than in controls, and TLR2 silencing restored IκBα levels to normal (Fig. 4B). In addition, IF results further confirmed these findings, showing increased MyD88 expression in the model group that was attenuated by TLR2 knockdown (Fig. 4C). The Co-IP results demonstrated successful immunoprecipitation of TLR2 and MyD88 in HCMECs, with reciprocal binding observed in both directions (TLR2 pulldown detected MyD88, and MyD88 pulldown detected TLR2), while the IgG control showed no nonspecific interaction. This confirmed a specific interaction between TLR2 and MyD88 proteins (Fig. 4D). Moreover, IP and Western blot results showed that TLR2 silence increased the protein level

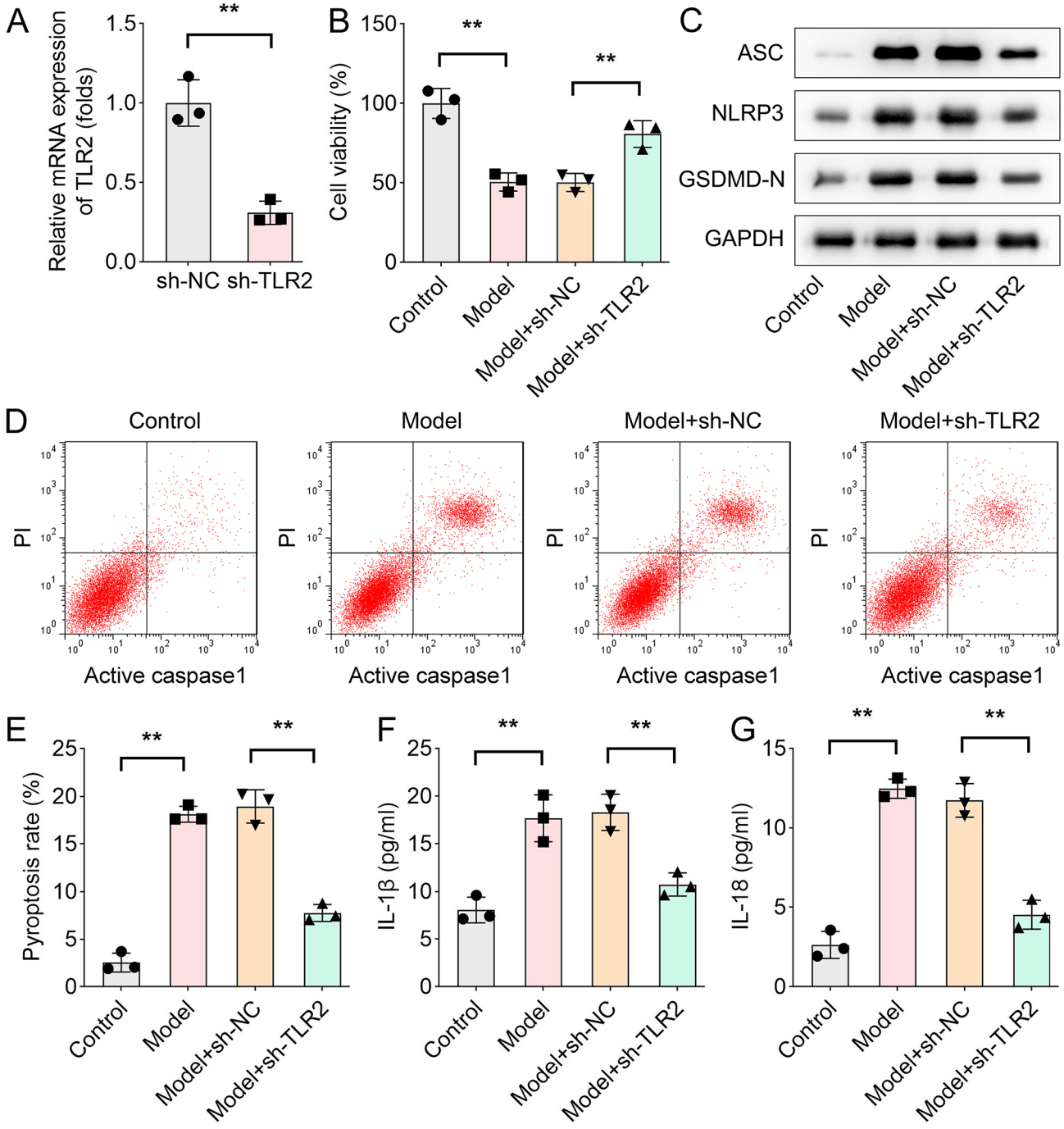

Fig. 3. Silencing TLR2 reversed the results in model group. **A**, The mRNA expression of TLR2 in sh-NC and sh-TLR2 groups was detected by reverse transcription-polymerase chain reaction; **B**, CCK-8 was used to analyze the cell viability in each group; **C**, Western blot was used to detect the protein levels of ASC, NLRP3, and GSDMD-N in each group; **D**, The pyroptosis of HCMECs in each group was analyzed using flow cytometry; **E**, The pyroptosis rate of HCMECs in each group was calculated; The levels of **F**, IL-1β and **G**, IL-18 were evaluated by ELISA. (**$p < 0.01$). TLR2, toll-like receptor 2; HCMECs, human cardiac microvascular endothelial cell line; CCK-8, cell counting kit-8; ASC, apoptosis-associated speck-like protein containing a caspase recruitment domain; NLRP3, NOD-like receptor family pyrin domain containing 3; GSDMD, gasdermin D; ELISA, enzyme-linked immunosorbent assay; IL, interleukin, sh-RNA, short hairpin RNA.

of MyD88 ubiquitination and decreased that of MyD88, while the results were reversed after MG132 treatment (Fig. 4E). These results demonstrated that TLR2 regulated the MyD88/NF-κB signaling pathway in DMA through both physical interaction with MyD88 and modulation of MyD88 protein stability via the ubiquitin-proteasome system.

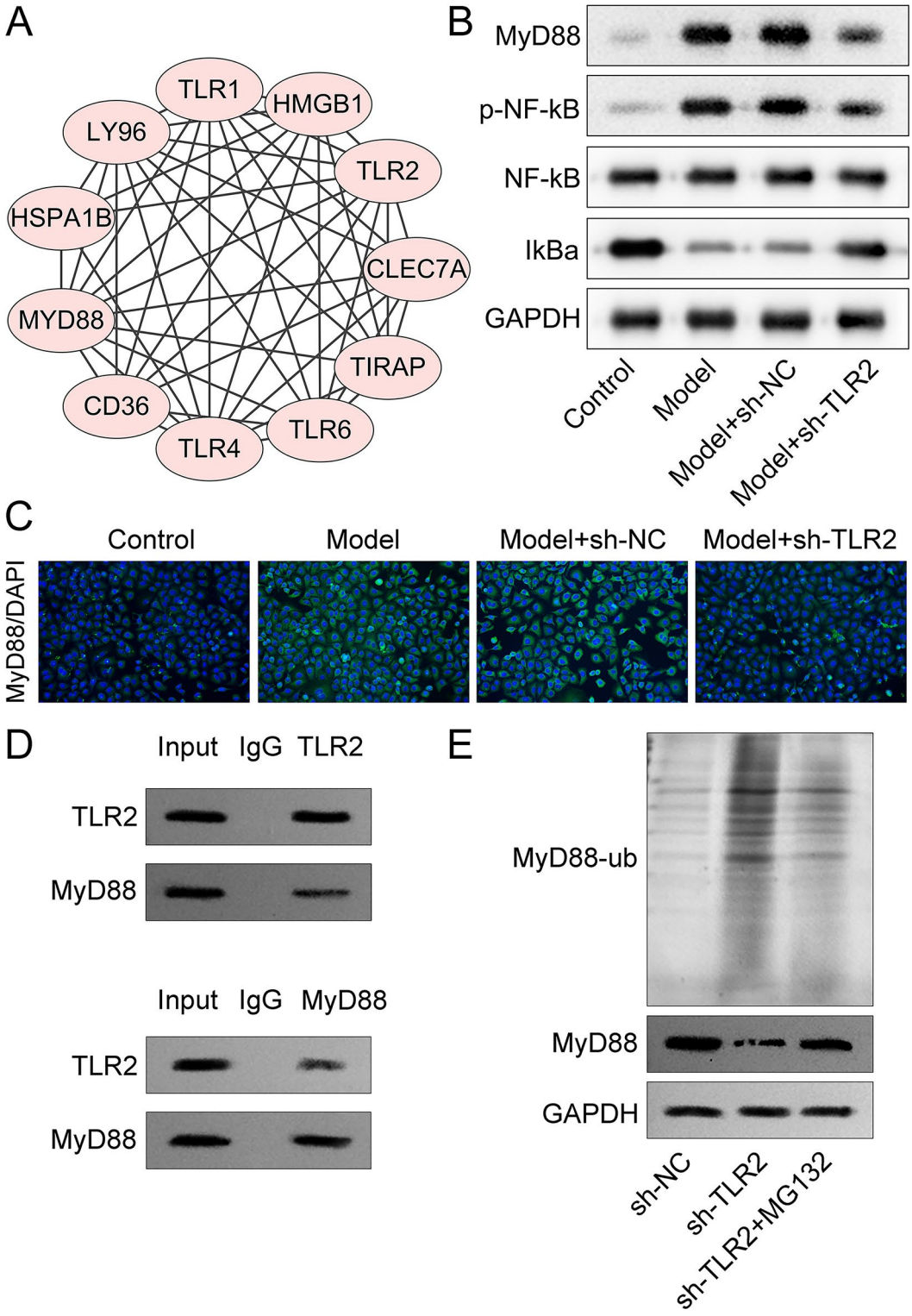

Fig. 4. Silencing TLR2 inhibited MyD88/NF-κB signaling pathway activation in HCMECs. **A**, STRING database was used to screen TLR2-related proteins; **B**, Western blot was performed to analyze the related protein levels of MyD88/NF-κB signaling pathway in each group; **C**, IF assay was performed to detect the expression of MyD88 in each group; **D**, Co-IP was used to assess the interaction between TLR2 and MyD88 in HCMECs; **E**, IP and Western blot were performed to measure the protein levels of MyD88-ub and MyD88 in HCMECs. TLR2, toll-like receptor 2; MyD88, myeloid differentiating factor 88; NF-κB, nuclear factor-kappaB; STRING, Search Tool for Recurring Instances of Neighbouring Genes; HCMECs, human cardiac microvascular endothelial cell line; IF, immunofluorescence; Co-IP, co-immunoprecipitation; ub, ubiquitination.

Treatment with BAY reversed the results in TLR2 overexpression group

Following transfection with the TLR2 overexpression vector, HCMECs exhibited a significant increase in TLR2 expression (Fig. 5A). Overexpression of TLR2 led to a reduction in cell viability, which was reversed upon treatment with the NF-κB inhibitor, BAY (Fig. 5B). Additionally, TLR2 overexpression elevated the protein levels of ASC, NLRP3, and GSDMD-N, effects that were counteracted by BAY treatment (Fig. 5C). Furthermore, the TLR2 overexpression group demonstrated an increased pyroptosis rate, higher concentrations of interleukin (IL)−1β and IL-18, and elevated protein levels of MyD88 and p-NF-κB. These effects were reversed in the presence of BAY (Figs. 5D-F). Conversely, the protein level of IκBα was reduced in the TLR2 overexpression group, and this decrease was restored following BAY treatment (Fig. 5G).

Silencing of TLR2 improved inflammation and atherosclerosis in diabetic mice

Subsequently, we further explored the role of TLR2 in vivo. Compared with the control group, the TLR2 expression in the aortic tissues of the model group was increased (Fig. 6A). Besides, the serum TLR2 concentration in the model group mice was also upregulated relative to the control group (Fig. 6B). In comparison to the AAV-shNC group, after TLR2 silence, the mRNA level of TLR2 was decreased in aortic tissues (Fig. 6C). ELISA results indicated that compared with the control group, the serum IL-18 and IL-1β concentrations were elevated. Besides, TLR2 inhibition decreased the serum contents of IL-18 and IL-1β relative to the model + AAV-shNC group (Figs. 6D-E). In addition, Oil Red O staining results demonstrated that the aortic tissues of model group mice showed increased lipid deposition compared with the control group. Moreover, after TLR2 silence, the lipid deposition was reduced in comparison to the model + AAV-shNC group (Fig. 6F). These data suggested that inhibition of TLR2 alleviated inflammation and atherosclerosis in diabetic mice.

Discussion

DMA is a critical health concern, as chronic hyperglycemia triggers a cascade of pathological events, such as endothelial dysfunction, enhanced inflammatory signaling, oxidative stress, and apoptotic cell death[19]. Among the key players in inflammatory diseases, TLRs have been extensively studied, particularly in conditions like coronary artery disease[20]. In this study, we observed elevated TLR2 levels in DMA patients. Although earlier studies have independently examined the role of TLR2 in DM and atherosclerosis[21], its specific contribution to DMA has not been thoroughly investigated. Additionally, prior findings have shown that TLR2 and TLR4 expression on monocytes is significantly elevated in type 1 DM patients with microvascular complications[21]. Notably, research by Miao et al.[22] indicates that the simultaneous inhibition of TLR2 and C-X-C motif chemokine receptor 4 (CXCR4) significantly attenuates and nearly reverses atherosclerosis induced by Chlamydia pneumoniae infection. Interestingly, TLR2 has potential crosstalk with other TLRs in related diseases. For instances, Lu et al.[23] reveal that TLR4 antagonist reduces early-stage atherosclerosis in diabetic apolipoprotein E-deficient mice. In addition, a previous study indicates that TLR9 plays a pivotal role in angiotensin II-induced atherosclerosis[24].

Furthermore, *in vitro*experiments revealed that HCMECs exposed to high glucose and oxLDL exhibited reduced cell viability, increased pyroptosis, elevated NLRP3-related protein expression, and higher concentrations of IL-1β and IL-18. These results suggested that increased TLR2 promoted DMA via activating NLRP3 inflammasome. The NLRP3 inflammasome plays a central role in inflammatory responses. This multiprotein complex facilitates the activation of caspase-1, leading to the maturation and release of IL-18 and IL-1β[19]. Extensive research has underscored the critical roles of the NLRP3 inflammasome, IL-1β, IL-18, and pyroptosis in the pathogenesis of conditions such as DM, atherosclerosis, and Alzheimer's disease[25–27], observations that are consistent with our findings. According to a review by Xue et al.[28], targeting the NLRP3 inflammasome represents a promising therapeutic approach for atherosclerosis. Furthermore, earlier studies have demonstrated that TLR2 knockout reduces the proinflammatory state in type 1 diabetes mellitus (T1DM)[29]. Furthermore, in various inflammatory conditions, including airway inflammation and *Selenium Attenuates S.* aureus-induced inflammation, TLR2 has been implicated in disease progression through its role in modulating NLRP3 inflammasome activation[30,31]. Similarly, a previous review reports that another TLRs family member, TLR9, activates NLRP3 inflammasomes and releases interleukin in various cardiovascular diseases, which eventually leads to tissue damage and inflammatory responses[32].

Additionally, NLRP3 inflammasome activation is often linked to the MyD88/NF-κB signaling pathway[33,34]. Our findings revealed that TLR2 inhibition normalized the elevated levels of MyD88 and p-NF-κB and restored the reduced levels of IκBα induced by high glucose and oxLDL, indicating that TLR2 exacerbates DMA through the MyD88/NF-κB pathway. Rescue experiments further supported these observations, as TLR2 overexpression reduced cell viability and enhanced pyroptosis, effects that were mitigated by the NF-κB inhibitor BAY. Notably, targeting the MyD88/NF-κB signaling pathway is considered a key therapeutic approach for various inflammatory vascular diseases[35,36]. Similar to our results, inhibiting the TLR2/MyD88/NF-κB pathway has been shown to exert protective effects in another DM-related complication, namely DM-induced renal injury[37]. Besides, the TLR4/MyD88/NF-κB signaling pathway is commonly activated in both DM and atherosclerosis, as supported by extensive research[38,39]. Additionally, TLR9 regulates NLRP3 inflammasome activation via the NF-kB signaling pathway in diabetic nephropathy[40].

In conclusion, our findings revealed that TLR2 significantly contributed to the progression of DMA by activating the NLRP3 inflammasome and the MyD88/NF-κB signaling pathway. These results highlighted TLR2 as a promising candidate for therapeutic intervention in DMA. The activation of these pathways underscores the potential for targeted treatments to mitigate disease progression.

However, several limitations should be acknowledged. First, our protein interaction analysis primarily relied on the STRING database prediction followed by targeted experimental validation, rather than comprehensive proteomic approaches such as immunoprecipitation-mass spectrometry (IP-MS). Future studies employing

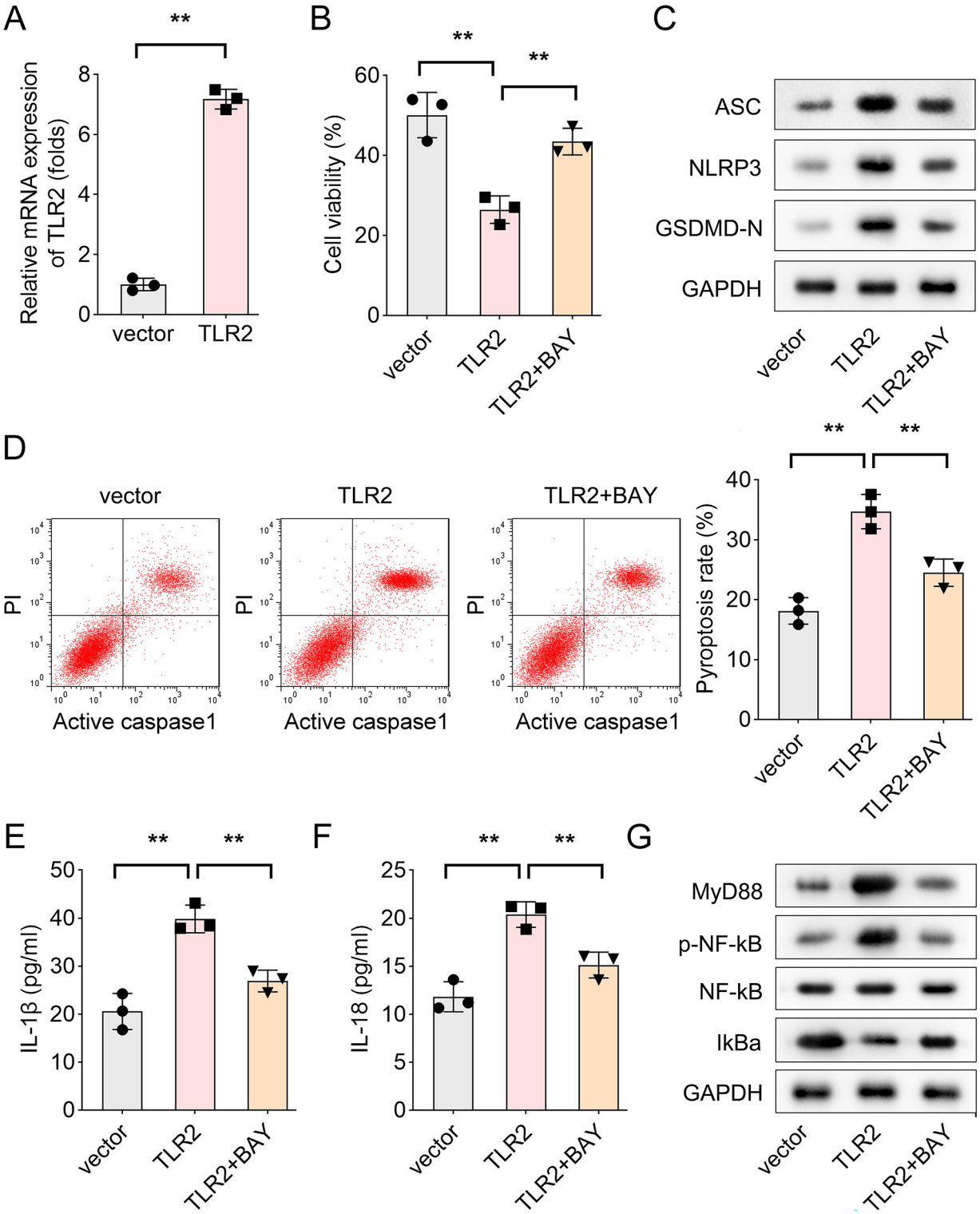

Fig. 5. Treatment with BAY reversed the results in TLR2 overexpression group. **A**, The expression of TLR2 in vector and TLR2 overexpression groups was detected by reverse transcription-polymerase chain reaction; **B**, The cell viability in each group was assessed by CCK-8 assay; **C**, Western blot was performed to analyze the protein levels of ASC, NLRP3, and GSDMD-N in each group; **D**, The pyroptosis rate in each group was evaluated by flow cytometry; The concentrations of **E**, IL-1β and **F**, IL-18 were analyzed by ELISA; **G**, The protein levels of MyD88, p-NF-κB, NF-κB, and IκBα were analyzed by Western blot. (**$p < 0.01$). TLR2, toll-like receptor 2; MyD88, myeloid differentiating factor 88; p-NF-κB, phospho-nuclear factor-kappaB; IκBα, inhibitor kappa B alpha; CCK-8, cell counting kit-8; ASC, apoptosis-associated speck-like protein containing a caspase recruitment domain; NLRP3, NOD-like receptor family pyrin domain containing 3; GSDMD, gasdermin D; ELISA, enzyme-linked immunosorbent assay; IL, interleukin.

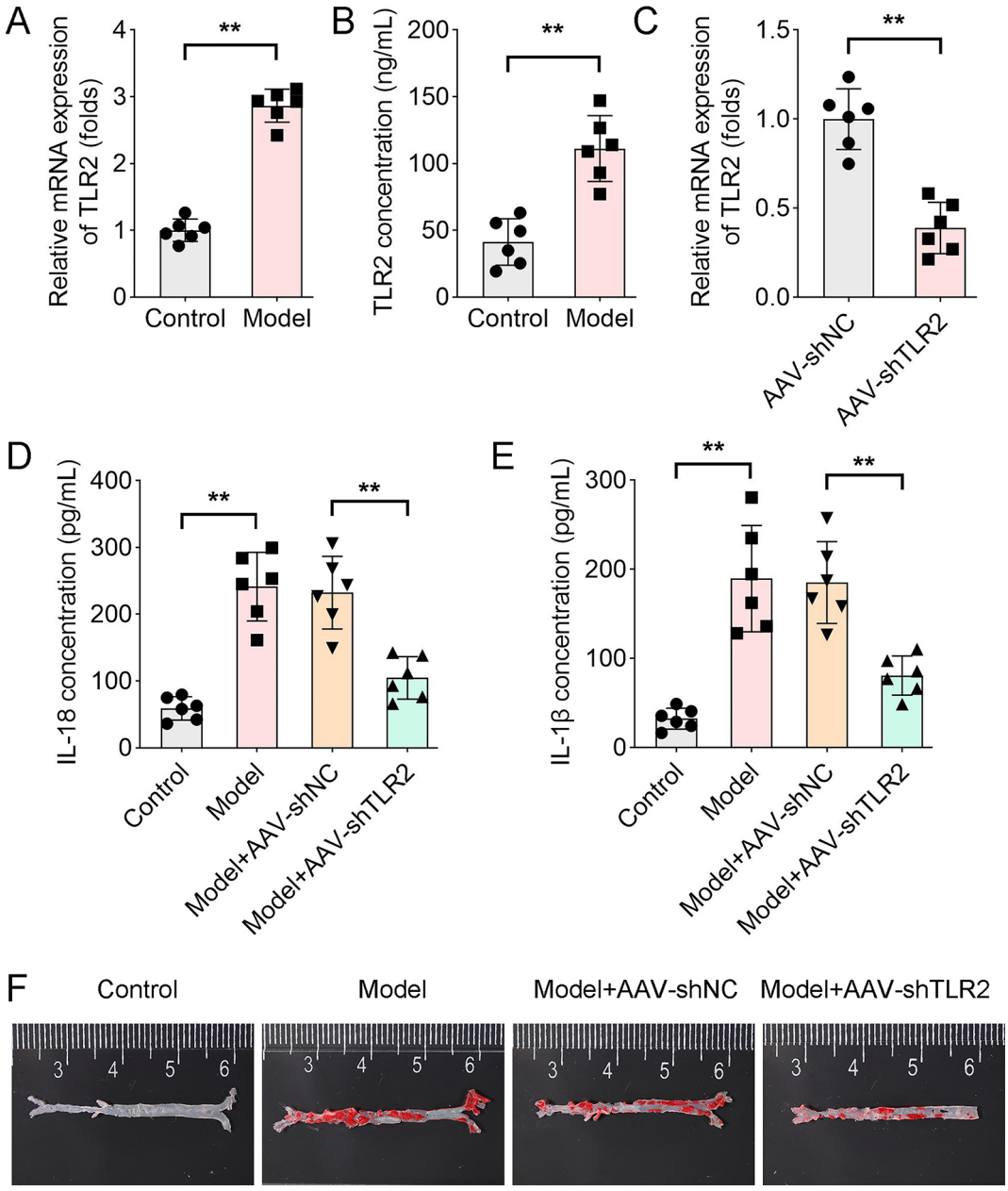

Fig. 6. Silencing of TLR2 improved inflammation and atherosclerosis in diabetic mice. **A**, The mRNA level of TLR2 in the control and the model group was analyzed by reverse transcription-polymerase chain reaction; **B**, Serum TLR2 concentration of TLR2 in the control and the model group was analyzed by ELISA; **C**, Reverse transcription-polymerase chain reaction was used to assess the TLR2 mRNA level; ELISA was performed to detect the serum concentrations of **D**, IL-18 and **E**, IL-1β in each group; **F**, Lipid deposition in the aortic tissues was determined using Oil Red O staining. ($^{**}p < 0.001$). TLR2, toll-like receptor 2; ELISA, enzyme-linked immunosorbent assay; IL, interleukin.

mass spectrometry-based proteomics could potentially identify additional components of this signaling complex. Second, the clinical sample size of this study is relatively small, which may affect the statistical power and general applicability of the research results. It is necessary for future studies to include a larger population to further verify the findings. Third, our *in vitro* model, while informative, may not fully recapitulate the complex microenvironment of human atherosclerotic plaques. Building on our findings, several promising research directions emerge: (1) Development of specific small-molecule TLR2 inhibitors for preclinical evaluation in DMA models; (2) Exploration of combination therapies simultaneously targeting TLR2 and downstream effectors (e.g., NLRP3 or NF-κB); (3) Investigation of stage-dependent TLR2 contributions using timed intervention studies; and (4) Optimization of tissue-specific delivery systems (e.g., nanoparticle-encapsulated TLR2 modulators) to enhance therapeutic precision. These approaches may accelerate the translation of TLR2-targeted therapies from bench to bedside.

Data availability

The datasets used and/or analysed during the current study are available from the corresponding author on reasonable request.

Received: 14 February 2025; Accepted: 30 April 2025
Published online: 10 May 2025

References

1. Cho, N. H. et al. IDF diabetes atlas: global estimates of diabetes prevalence for 2017 and projections for 2045. *Diabetes Res. Clin. Pract.* **138**, 271–281 (2018).
2. Yan, Y. et al. HucMSC Exosome-Derived GPX1 is required for the recovery of hepatic oxidant injury. *Mol. Ther.* **25**, 465–479 (2017).
3. Sun, Y. et al. The utility of exosomes in diagnosis and therapy of diabetes mellitus and associated complications. *Front. Endocrinol. (Lausanne).* **12**, 756581 (2021).
4. Miname, M. H. & Santos, R. D. Reducing cardiovascular risk in patients with Familial hypercholesterolemia: risk prediction and lipid management. *Prog Cardiovasc. Dis.* **62**, 414–422 (2019).
5. Taleb, S. Inflammation in atherosclerosis. *Arch. Cardiovasc. Dis.* **109**, 708–715 (2016).
6. Yuan, T. et al. New insights into oxidative stress and inflammation during diabetes Mellitus-Accelerated atherosclerosis. *Redox Biol.* **20**, 247–260 (2019).
7. Gorecki, A. M., Anyaegbu, C. C. & Anderton, R. S. TLR2 and TLR4 in Parkinson's disease pathogenesis: the environment takes a toll on the gut. *Transl Neurodegener*. **10**, 47 (2021).
8. Chen, F., Chen, Z. Q., Zhong, G. L. & Zhu, J. J. Nicorandil inhibits TLR4/MyD88/NF-kappaB/NLRP3 signaling pathway to reduce pyroptosis in rats with myocardial infarction. *Exp. Biol. Med. (Maywood)*. **246**, 1938–1947 (2021).
9. Li, B., Xia, Y. & Hu, B. Infection and atherosclerosis: TLR-dependent pathways. *Cell. Mol. Life Sci.* **77**, 2751–2769 (2020).
10. Hardigan, T., Hernandez, C., Ward, R., Hoda, M. N. & Ergul, A. TLR2 knockout protects against Diabetes-Mediated changes in cerebral perfusion and cognitive deficits. *Am. J. Physiol. Regul. Integr. Comp. Physiol.* **312**, R927–R937 (2017).
11. Radzyukevich, Y. V., Kosyakova, N. I. & Prokhorenko, I. R. Impact of Comorbidity of Bronchial Asthma and Type 2 Diabetes Mellitus on the Expression and Functional Activity of TLR2 and TLR4 Receptors. *Life (Basel)*. 13, (2023).
12. Beutler, B. & Inferences Questions and possibilities in Toll-like receptor signalling. *Nature* **430**, 257–263 (2004).
13. Yu, H., Lin, L., Zhang, Z., Zhang, H. & Hu, H. Targeting NF-kappaB pathway for the therapy of diseases: mechanism and clinical study. *Signal. Transduct. Target. Ther.* **5**, 209 (2020).
14. Choudhury, R. P. et al. Arterial effects of Canakinumab in patients with atherosclerosis and type 2 diabetes or glucose intolerance. *J. Am. Coll. Cardiol.* **68**, 1769–1780 (2016).
15. Guo, X. L., Wang, J. W., Tu, M. & Wang, W. Perirenal fat thickness as a superior Obesity-Related marker of subclinical carotid atherosclerosis in type 2 diabetes mellitus. *Front. Endocrinol. (Lausanne)*. **14**, 1276789 (2023).
16. Hu, W. T. et al. IL-33 enhances proliferation and invasiveness of decidual stromal cells by Up-Regulation of CCL2/CCR2 via NF-kappaB and ERK1/2 signaling. *Mol. Hum. Reprod.* **20**, 358–372 (2014).
17. Wang, Y. W. et al. HIF-1alpha-regulated lncRNA-TUG1 promotes mitochondrial dysfunction and pyroptosis by directly binding to FUS in myocardial infarction. *Cell. Death Discov.* **8**, 178 (2022).
18. Zhang, Y. et al. Fufang Zhenzhu Tiaozhi (FTZ) capsule ameliorates Diabetes-Accelerated atherosclerosis via suppressing YTHDF2-mediated m(6)A modification of SIRT3 mRNA. *J. Ethnopharmacol.* **317**, 116766 (2023).
19. Ye, J. et al. Diabetes mellitus promotes the development of atherosclerosis: the role of NLRP3. *Front. Immunol.* **13**, 900254 (2022).
20. Roshan, M. H., Tambo, A. & Pace, N. P. The Role of TLR2, TLR4, and TLR9 in the Pathogenesis of Atherosclerosis. *Int J Inflam.* 1532832 (2016). (2016).
21. Devaraj, S., Jialal, I., Yun, J. M. & Bremer, A. Demonstration of increased Toll-Like receptor 2 and Toll-Like receptor 4 expression in monocytes of type 1 diabetes mellitus patients with microvascular complications. *Metabolism* **60**, 256–259 (2011).
22. Miao, G. et al. TLR2/CXCR4 coassociation facilitates Chlamydia Pneumoniae Infection-Induced atherosclerosis. *Am. J. Physiol. Heart Circ. Physiol.* **318**, H1420–H1435 (2020).
23. Lu, Z., Zhang, X., Li, Y., Jin, J. & Huang, Y. TLR4 antagonist reduces Early-Stage atherosclerosis in diabetic Apolipoprotein E-deficient mice. *J. Endocrinol.* **216**, 61–71 (2013).
24. Fukuda, D. et al. Toll-Like receptor 9 plays a pivotal role in angiotensin II-Induced atherosclerosis. *J. Am. Heart Assoc.* **8**, e10860 (2019).
25. Strowig, T., Henao-Mejia, J., Elinav, E. & Flavell, R. Inflammasomes in health and disease. *Nature* **481**, 278–286 (2012).
26. Ding, S. et al. Modulatory mechanisms of the NLRP3 inflammasomes in diabetes. *Biomolecules* **9**, (2019).
27. Grebe, A., Hoss, F. & Latz, E. NLRP3 inflammasome and the IL-1 pathway in atherosclerosis. *Circ. Res.* **122**, 1722–1740 (2018).
28. Xue, X. et al. Hydroxysafflor yellow A, a natural compound from Carthamus Tinctorius L with good effect of alleviating atherosclerosis. *Phytomedicine* **91**, 153694 (2021).
29. Jialal, I. & Kaur, H. The role of Toll-Like receptors in Diabetes-Induced inflammation: implications for vascular complications. *Curr. Diab Rep.* (2012).
30. Wu, H. M., Zhao, C. C., Xie, Q. M., Xu, J. & Fei, G. H. TLR2-Melatonin feedback loop regulates the activation of NLRP3 inflammasome in murine allergic airway inflammation. *Front. Immunol.* **11**, 172 (2020).
31. Wei, M. J. et al. Selenium attenuates S. Aureus-Induced inflammation by regulation TLR2 signaling pathway and NLRP3 inflammasome in RAW 264.7 macrophages. *Biol. Trace Elem. Res.* **200**, 761–767 (2022).
32. Li, D. et al. Novel insights and current evidence for mechanisms of atherosclerosis: mitochondrial dynamics as a potential therapeutic target. *Front. Cell. Dev. Biol.* **9**, 673839 (2021).
33. Yang, B. Y. et al. Datura Metel L. Ameliorates Imiquimod-Induced Psoriasis-Like dermatitis and inhibits inflammatory cytokines production through TLR7/8-MyD88-NF-kappaB-NLRP3 inflammasome pathway. *Molecules* **24**, (2019).
34. Jiang, S. et al. Proteopathic Tau primes and activates Interleukin-1beta via Myeloid-Cell-Specific MyD88- and NLRP3-ASC-inflammasome pathway. *Cell. Rep.* **36**, 109720 (2021).
35. Wang, L. et al. Acupuncture Attenuates Inflammation in Microglia of Vascular Dementia Rats by Inhibiting miR-93-Mediated TLR4/MyD88/NF-kappaB Signaling Pathway. *Oxid. Med. Cell. Longev.* 8253904 (2020). (2020).
36. Huang, L. et al. PCSK9 promotes endothelial dysfunction during Sepsis via the TLR4/MyD88/NF-kappaB and NLRP3 pathways. *Inflammation* **46**, 115–128 (2023).
37. Xu, Y. Y., Chen, T., Ding, H., Chen, Q. & Fan, Q. L. Melatonin inhibits circadian gene DEC1 and TLR2/MyD88/NF-kappaB signaling pathway to alleviate renal injury in type 2 diabetic mice. *Acta Diabetol.* **61**, 1455–1474 (2024).
38. Li, Y. et al. Qing-Xue-Xiao-Zhi formula attenuates atherosclerosis by inhibiting macrophage lipid accumulation and inflammatory response via TLR4/MyD88/NF-kappaB pathway regulation. *Phytomedicine* **93**, 153812 (2021).
39. Liu, Y. et al. Lycopene ameliorates islet function and Down-Regulates the TLR4/MyD88/NF-kappaB pathway in diabetic mice and Min6 cells. *Food Funct.* **14**, 5090–5104 (2023).

40. Shen, J., Dai, Z., Li, Y., Zhu, H. & Zhao, L. TLR9 regulates NLRP3 inflammasome activation via the NF-kB signaling pathway in diabetic nephropathy. *Diabetol. Metab. Syndr.* **14**, 26 (2022).

Author contributions

All authors participated in the design, interpretation of the studies and analysis of the data and review of the manuscript. S C drafted the work and revised it critically for important intellectual content; M X was responsible for the acquisition, analysis and interpretation of data for the work; Y L made substantial contributions to the conception or design of the work. All authors read and approved the final manuscript.

Funding

The work was supported by Scientific Research Project of Hubei Provincial Health Commission under grant number WJ2021 F038.

Declarations

Ethics approval and consent to participate

This study was performed in line with the principles of the Declaration of Helsinki. Approval was granted by the Ethics Committee of Renmin Hospital, Hubei University of Medicine. Informed consent was obtained from all individual participants included in the study. All methods were carried out in accordance with relevant guidelines and regulations.

Competing interests

The authors declare no competing interests.

Additional information

Supplementary Information The online version contains supplementary material available at https://doi.org/10.1038/s41598-025-00843-4.

Correspondence and requests for materials should be addressed to Y.L.

Reprints and permissions information is available at www.nature.com/reprints.

Publisher's note Springer Nature remains neutral with regard to jurisdictional claims in published maps and institutional affiliations.